Design of Two-Dimensional FIR Digital Filters by Using the Singular-Value Decomposition

WU-SHENG LU, MEMBER, IEEE, HUI-PING WANG, STUDENT MEMBER, IEEE, AND ANDREAS ANTONIOU, FELLOW, IEEE

***Abstract*—The singular-value decomposition (SVD) is applied in the design of two-dimensional (2-D) FIR digital filters. It is shown that three realizations are possible, namely, a direct realization, a modified version of the direct realization, and a realization based on the combined application of the SV and LU decompositions. Each of the three realizations consists of a parallel arrangement of cascaded pairs of 1-D filters; hence extensive parallel processing and pipelining can be applied. The 1-D FIR filters can be designed using well-known standard design methods and by using linear-phase filters, linear-phase causal 2-D filters can be designed which are suitable for real-time or quasi-real-time applications. The three realizations are compared and it is shown that the realization based on the SV and LU decompositions leads to the lowest approximation error and involves the smallest number of multiplications. The SVD, the McClellan transformation, and the 2-D window design methods are used to design a bandpass and a fan filter, and the results obtained are compared.**

I. Introduction

The design of 2-D digital filters by using the singular-value decomposition (SVD) and other similar decompositions has been investigated by a number of researchers [1]–[6]. This design approach has several advantages. First, the design can be accomplished by designing a set of 1-D subfilters and, therefore, the many well-established techniques for the design of 1-D filters can be employed; second, the resulting 2-D filter is stable if the 1-D subfilters employed are stable; and third, the 1-D subfilters form a parallel structure which allows extensive parallel processing. As pointed out in [3], the SVD approach can be used for the design of either infinite-impulse response (IIR) or finite-impulse response (FIR) 2-D filters. While high selectivity can be achieved by using low-order IIR designs for the parallel 1-D subfilters, zero phase is required for each subfilter. This necessitates data transpositions at the inputs and outputs of subfilters and, as a result, the usefulness of these designs is limited to nonreal-time applications, where the delay introduced in the processing is unimportant.

In this paper, the SVD approach reported in [3] is applied in conjunction with 1-D FIR techniques for the design of 2-D quadrantally-symmetric FIR filters. It is shown that three realizations are possible and in each case, causal, linear-phase designs can easily be obtained. The first realization is based on the direct application of the SVD to a matrix representing the required amplitude response and as in the IIR realizations reported in [3], the number of parallel filter sections is equal to the number of singular values used in the design. In practice, a designer would attempt to keep the error introduced by the application of the SVD as low as possible by using as many as singular values as possible in the design. However, as more and more singular values are used, more and more parallel sections are required which increase the computational complexity or the cost of hardware involved in the implementation. The second realization is a modified version of the first which takes advantage of the symmetry of the impulse response of a linear-phase 2-D FIR filter. The design is reformulated in terms of the singular values of a matrix C of rank r_c, where r_c does not exceed half of the order of the 1-D FIR filters used. This allows the designer to eliminate the error introduced by the application of the SVD using a smaller number of parallel sections. The third realization is, in effect, a modified version of the second realization which has the same advantage with respect to the number of parallel sections required to eliminate the error introduced by the application of the SVD and has, in addition, the advantage that the number of multiplications can be reduced further through the use of the LU decomposition.

In all three realization methods, the outcome is a 2-D causal linear-phase parallel filter which is suitable for real-time or quasi-real-time applications.

II. Design

A 2-D FIR digital filter with support in the rectangle defined by $-(N_i-1)/2 \leqslant n_i \leqslant (N_i-1)/2$, $i=1, 2$, can be characterized by the transfer function

$$H(z_1, z_2) = \sum_{n_1=-(N_1-1)/2}^{(N_1-1)/2} \sum_{n_2=-(N_2-1)/2}^{(N_2-1)/2} h(n_1, n_2) z_1^{-n_1} z_2^{-n_2} \tag{1}$$

where $h(n_1, n_2)$ is its impulse response. If $h(n_1, n_2)$ is real,

Manuscript received May 26, 1988; revised May 22, 1989. This paper was recommended by Associate Editor Y. C. Jenq.
The authors are with the Department of Electrical and Computer Engineering, University of Victoria, Victoria, B.C., Canada V8W 2Y2.
IEEE Log Number 8931719.

and

$$h(n_1, n_2) = h(-n_1, -n_2)$$

then the frequency response of the filter

$$H(e^{j\omega_1 T_1}, e^{j\omega_2 T_2}) = \sum_{n_1=-(N_1-1)/2}^{(N_1-1)/2} \sum_{n_2=-(N_2-1)/2}^{(N_2-1)/2} h(n_1, n_2) e^{-j\omega_1 n_1 T_1} e^{-j\omega_2 n_2 T_2} = X(\omega_1, \omega_2)$$

is a real function which is even with respect to ω_1 and ω_2.

The transfer function given in (1) can be rewritten as

$$H(z_1, z_2) = \sum_{i=1}^{K} F_i(z_1) G_i(z_2) \tag{2}$$

where $F_i(z_1)$ and $G_i(z_2)$ are transfer functions of 1-D subfilters in the z_1 and z_2 domains, respectively. If these subfilters are FIR filters with support in the rectangle defined by $-(N_i-1)/2 \leqslant n_i \leqslant (N_i-1)/2$, $i = 1,2$, we have

$$F_i(z_1) = \sum_{n_1=-(N_1-1)/2}^{(N_1-1)/2} f_i(n_1) z_1^{-n_1} \tag{3}$$

and

$$G_i(z_2) = \sum_{n_2=-(N_2-1)/2}^{(N_2-1)/2} g_i(n_2) z_2^{-n_2} \tag{4}$$

and if $F_i(z_1)$ and $G_i(z_2)$ are assumed to represent zero-phase filters, then their frequency responses are given by

$$F_i(e^{j\omega_1 T_1}) = \sum_{n_1=-(N_1-1)/2}^{(N_1-1)/2} f_i(n_1) e^{-j\omega_1 n_1 T_1} = \Phi_i(\omega_1) \tag{5}$$

and

$$G_i(e^{j\omega_2 T_2}) = \sum_{n_2=-(N_2-1)/2}^{(N_2-1)/2} g_i(n_2) e^{-j\omega_2 n_2 T_2} = \Gamma_i(\omega_2) \tag{6}$$

where $\Phi_i(\omega_1)$ and $\Gamma_i(\omega_2)$ are real functions which are even with respect to ω_1 and ω_2, respectively. Consequently, from (2) to (6) the frequency response for a quadrantally-symmetric 2-D filter can be written as

$$\begin{aligned} H(e^{j\omega_1 T_1}, e^{j\omega_2 T_2}) &= \sum_{i=1}^{K} F_i(e^{j\omega_1 T_1}) G_i(e^{j\omega_2 T_2}) \\ &= \sum_{i=1}^{K} \Phi_i(\omega_1) \Gamma_i(\omega_2) \\ &= X(\omega_1, \omega_2). \end{aligned} \tag{7}$$

Now assume that matrix $A = \{a_{l,m}\}$ represents a desired frequency response, i.e.,

$$X\left(\frac{\pi\mu_l}{T_1}, \frac{\pi\nu_m}{T_2}\right) = a_{l,m}, \qquad 1 \leqslant l \leqslant L; 1 \leqslant m \leqslant M \tag{8}$$

where μ_l and ν_m are normalized frequencies such that

$$\mu_l = \frac{l-1}{L-1}; \qquad \nu_m = \frac{m-1}{M-1}$$

and $0 \leqslant \mu_l \leqslant 1$, $0 \leqslant \nu_m \leqslant 1$. The SVD of A gives

$$A = \sum_{i=1}^{r} \sigma_i \boldsymbol{u}_i \boldsymbol{v}_i^T = \sum_{i=1}^{r} \tilde{\boldsymbol{u}}_i \tilde{\boldsymbol{v}}_i^T \tag{9}$$

where σ_i are the singular values of A such that $\sigma_1 \geqslant \sigma_2 \geqslant \cdots \geqslant \sigma_r > 0$, r is the rank of A, and $\tilde{\boldsymbol{u}}_i = \sigma_i^{1/2} \boldsymbol{u}_i$, $\tilde{\boldsymbol{v}}_i = \sigma_i^{1/2} \boldsymbol{v}_i$.

On assuming that $\tilde{\boldsymbol{u}}_i$ and $\tilde{\boldsymbol{v}}_i$ are sampled versions of the frequency responses of the 1-D filters characterized by $F_i(z_1)$ and $G_i(z_2)$, respectively, a 2-D zero-phase FIR filter can be designed by designing two sets of 1-D zero-phase FIR subfilters characterized by $F_i(z_1)$ and $G_i(z_2)$, where $1 \leqslant i \leqslant r$. A 2-D causal linear-phase filter can readily be obtained by shifting the impulse response by $(N_1-1)/2$ and $(N_2-1)/2$ with respect to the n_1 axis and n_2 axis, respectively. This can be accomplished by multiplying $F_i(z_1)$ and $G_i(z_2)$ by $z_1^{-(N_1-1)/2}$ and $z_2^{-(N_2-1)/2}$, respectively.

The design of the 2-D filter can be completed by using any one of the standard methods for the design of 1-D FIR filters. Using the Fourier series method in conjunction with window techniques [7], designs can be obtained very quickly with a small amount of computational effort. These designs are not optimal although the approximation error can be made arbitrarily small by increasing the order of the 1-D filters used. On the other hand, by using methods based on the Reméz algorithm [8], it may be possible to obtain optimal designs although a large amount of computation would be required.

III. SVD Realizations

Three distinct realizations are possible through the application of the SVD, which will be referred to as the direct-SVD realization, the modified-SVD realization, and the SVD-LUD realization.

A. Direct-SVD Realization

The direct-SVD realization is obtained by using the design method described in Section II. The steps involved are as follows.

1) Specify the desired amplitude response and thereby obtain the corresponding sampled amplitude-response matrix A given in (8).

2) Decompose matrix A using the SVD as in (9) to get $\tilde{\boldsymbol{u}}_i$ and $\tilde{\boldsymbol{v}}_i$, where $1 \leqslant i \leqslant r$.

3) Design K 2-D FIR filters, each of which is obtained by designing two 1-D zero-phase FIR filters characterized by transfer functions $F_i(z_1)$ and $G_i(z_2)$ corresponding to the desired amplitude responses $\tilde{\boldsymbol{u}}_i$ and $\tilde{\boldsymbol{v}}_i$, respectively, where $1 \leqslant i \leqslant K$ and $1 \leqslant K \leqslant r$.

4) Obtain the resulting 2-D zero-phase transfer function through (2).

5) Multiply the resulting 2-D zero-phase transfer function by $z_1^{-(N-1)/2}$ and $z_2^{-(N-1)/2}$, respectively, to obtain the linear-phase 2-D transfer function.

If $N_1 = N_2 = N$, the number of the multiplications needed in the direct SVD realization is $2K\overline{N}$ where

$$\overline{N} = \begin{cases} N/2, & \text{if } N \text{ is even} \\ (N+1)/2, & \text{if } N \text{ is old} \end{cases}$$

is the number of multiplications needed in the implementation of a 1-D FIR filter. Integer K is the number of singular values that must be used in the design to reduce the approximation error introduced by the SVD to a satisfactory level.

B. Modified-SVD Realization

The modified-SVD realization can be obtained by manipulating the transfer function of the 2-D filter. From (2) to (4), we can write

$$\begin{aligned} H(z_1, z_2) &= \sum_{i=1}^{K} \left[\sum_{n_1=-(N-1)/2}^{(N-1)/2} f_i(n_1) z_1^{-n_1} \right] \cdot \left[\sum_{n_2=-(N-1)/2}^{(N-1)/2} g_i(n_2) z_2^{-n_2} \right] \\ &= \sum_{n_1=-(N-1)/2}^{(N-1)/2} \sum_{n_2=-(N-1)/2}^{(N-1)/2} \left[\sum_{i=1}^{K} f_i(n_1) g_i(n_2) \right] z_1^{-n_1} z_2^{-n_2} \\ &= \sum_{n_1=-(N-1)/2}^{(N-1)/2} \sum_{n_2=-(N-1)/2}^{(N-1)/2} c(n_1, n_2) z_1^{-n_1} z_2^{-n_2} \end{aligned} \tag{10}$$

where

$$c(n_1, n_2) = \sum_{i=1}^{K} f_i(n_1) g_i(n_2). \tag{11}$$

The SVD of matrix $\boldsymbol{C} = \{c(n_1, n_2)\}$ can be written as

$$\begin{aligned} \boldsymbol{C} &= \sum_{i=1}^{r_c} \sigma_{ci} \boldsymbol{u}_{ci} \boldsymbol{v}_{ci}^T \\ &= \sum_{i=1}^{r_c} \tilde{\boldsymbol{u}}_{ci} \tilde{\boldsymbol{v}}_{ci}^T \end{aligned} \tag{12}$$

where r_c is the rank of $\boldsymbol{C}$. Now if all the singular values of $\boldsymbol{C}$ for $i > K_c$ can be neglected, we can write

$$\boldsymbol{C} \approx \sum_{i=1}^{K_c} \tilde{\boldsymbol{u}}_{ci} \tilde{\boldsymbol{v}}_{ci}^T \tag{13}$$

and on combining (10) and (13), we have

$$\begin{aligned} H(z_1, z_2) &\approx \sum_{n_1=-(N-1)/2}^{(N-1)/2} \sum_{n_2=-(N-1)/2}^{(N-1)/2} \sum_{i=1}^{K_c} \cdot \tilde{u}_{ci}(n_1) \tilde{v}_{ci}(n_2) z_1^{-n_1} z_2^{-n_2} \\ &\approx \sum_{i=1}^{K_c} \tilde{F}_{ci}(z_1) \tilde{G}_{ci}(z_2) = \hat{H}(z_1, z_2) \end{aligned} \tag{14}$$

where

$$\tilde{F}_{ci}(z_1) = \sum_{n_1=-(N-1)/2}^{(N-1)/2} \tilde{u}_{ci}(n_1) z_1^{-n_1}$$

and

$$\tilde{G}_{ci}(z_2) = \sum_{n_2=-(N-1)/2}^{(N-1)/2} \tilde{v}_{ci}(n_2) z_2^{-n_2}.$$

Therefore, a realization can be obtained by connecting K_c $(1 \leqslant K_c \leqslant r_c)$ 2-D zero-phase filters in parallel, where each 2-D filter consists of two cascaded 1-D FIR filters represented by $\tilde{F}_{ci}(z_1)$ and $\tilde{G}_{ci}(z_2)$.

A step-by-step procedure for the modified-SVD realization starts with steps (1)–(4) given in Section III-A and concludes with the following additional steps.

5) Form coefficient matrix $\boldsymbol{C}$ by (11).

6) Perform the SVD on matrix $\boldsymbol{C}$ to obtain vectors $\tilde{\boldsymbol{u}}_{ci}$ and $\tilde{\boldsymbol{v}}_{ci}$, $1 \leqslant i \leqslant r_c$, as in (12) and retain the vectors corresponding to the K_c most significant singular values.

7) Obtain the 2-D zero-phase transfer function through (14).

By (11)

$$\boldsymbol{C} = \sum_{i=1}^{K} \boldsymbol{f}_i \boldsymbol{g}_i^T = [\boldsymbol{f}_1 \cdots \boldsymbol{f}_K][\boldsymbol{g}_1 \cdots \boldsymbol{g}_K]^T$$

where

$$\boldsymbol{f}_i = [f_i(-(N-1)/2) \cdots f_i((N-1)/2)]^T$$

$$\boldsymbol{g}_i = [g_i(-(N-1)/2) \cdots g_i((N-1)/2)]^T.$$

Hence it follows that the rank of $\boldsymbol{C}$ satisfies the inequality $r_c \leqslant K$. Moreover, since each $\boldsymbol{f}_i$ and $\boldsymbol{g}_i$ are mirror-image symmetric, matrix $\boldsymbol{C}$ is quadrantally symmetric (see (A.1) in Appendix A). Consequently, there are at most $\overline{N}$ linearly independent row (or column) vectors in $\boldsymbol{C}$ and, therefore,

$$r_c \leqslant \min(\overline{N}, K). \tag{15}$$

In the modified-SVD realization, vectors $\tilde{\boldsymbol{u}}_{ci}$ and $\tilde{\boldsymbol{v}}_{ci}$ in (12) are all mirror-image symmetric, as shown in Appendix A. Consequently, $\tilde{F}_{ci}(z_1)$ and $\tilde{G}_{ci}(z_2)$ represent 1-D zero-phase FIR filters which can be readily designed using one of the standard methods. A 2-D, causal, linear-phase realization can be obtained by multiplying $\tilde{F}_{ci}(z_1)$ and $\tilde{G}_{ci}(z_2)$ by $z_1^{-(N-1)/2}$ and $z_2^{-(N-1)/2}$, respectively.

The number of multiplications required by the modified-SVD realization is $2K_c\overline{N}$. If $K < \overline{N}$ then from (15) we have $K_c \leqslant r_c \leqslant K$ and, therefore, the modified-SVD realization is more economical than the direct-SVD realization. If $K > \overline{N}$, we have $K_c \leqslant r_c \leqslant \overline{N}$ and, once again, the modified-SVD realization is more economical than the direct-SVD realization. In the latter case, the modified-SVD realization has the additional advantage that the value of K can be increased to r, the number of singular values in $\boldsymbol{A}$, without increasing the number of multiplications. Consequently, the approximation error can be reduced further at no additional cost.

C. SVD-LUD Realization

The SVD-LUD realization is similar to the modified-SVD realization but, as will be shown, it is more economical in terms of the number of multiplications required. Instead of decomposing $\boldsymbol{C}$ using the SVD, the LUD is used [9] to give

$$\boldsymbol{C} = \boldsymbol{L}_c \boldsymbol{U}_c \tag{16}$$

where $\boldsymbol{L}_c$ and $\boldsymbol{U}_c \in \boldsymbol{R}^{N \times N}$ are lower and upper triangular matrices, respectively. Since matrix $\boldsymbol{C}$ given by (11) is quadrantally symmetric, it can be shown that $\boldsymbol{L}_c = \{l_{i,j}\}$ and $\boldsymbol{U}_c = \{u_{i,j}\}$ satisfy the relations:

$$\begin{aligned} l_{i,j} &= l_{N-i+1,j}, && \text{for } 1 \leqslant i,\ j \leqslant N \\ l_{i,j} &= 0, && \text{for } j > r_c \\ l_{i,j} &= 0, && \text{for } i < j;\ j \leqslant r_c \end{aligned}$$

and

$$\begin{aligned} u_{i,j} &= u_{i,N-j+1}, && \text{for } 1 \leqslant i,\ j \leqslant N \\ u_{i,j} &= 0, && \text{for } i > r_c \\ u_{i,j} &= 0, && \text{for } j < i;\ i \leqslant r_c \end{aligned}$$

respectively, i.e., $\boldsymbol{L}_c$ and $\boldsymbol{U}_c$ have the forms:

$$\boldsymbol{L}_c = \begin{bmatrix} * & 0 & & & \cdots & 0 \\ * & * & 0 & & \cdots & 0 \\ * & \cdots & * & 0 & \cdots & 0 \\ \vdots & & \vdots & \vdots & & \vdots \\ * & \cdots & * & 0 & \cdots & 0 \\ * & * & 0 & & \cdots & 0 \\ * & 0 & & & \cdots & 0 \end{bmatrix}$$

and

$$\boldsymbol{U}_c = \begin{bmatrix} * & * & * & \cdots & * & * & * \\ 0 & * & \vdots & & \vdots & * & 0 \\ & 0 & * & \cdots & * & 0 & \\ & & 0 & \cdots & 0 & & \\ \vdots & \vdots & \vdots & & \vdots & \vdots & \vdots \\ 0 & 0 & 0 & \cdots & 0 & 0 & 0 \end{bmatrix}$$

respectively, (see Appendix B) where the nonzero columns (rows) in $\boldsymbol{L}_c(\boldsymbol{U}_c)$ are also mirror-image symmetric.

Now if we let $\boldsymbol{Z}_i = [z_i^{(N-1)/2}, \cdots, 1 \cdots, z_i^{-(N-1)/2}]$, $i = 1, 2$, then (14) can be written as

$$\begin{aligned} \hat{H}(z_1, z_2) &= \boldsymbol{Z}_1 \boldsymbol{L}_c \boldsymbol{U}_c \boldsymbol{Z}_2^T \\ &= \sum_{i=1}^{K_c} L_{ci}(z_1) U_{ci}(z_2) \end{aligned} \tag{17}$$

where $1 \leqslant K_c \leqslant r_c$ and

$$L_{ci}(z_1) = \sum_{n_1 = i-(N+1)/2}^{(N+1)/2-i} l_{n_1,i} z_1^{-n_1}$$

and

$$U_{ci}(z_2) = \sum_{n_2 = i-(N+1)/2}^{(N+1)/2-i} u_{i,n_2} z_2^{-n_2}.$$

A 2-D causal linear-phase realization can be obtained by multiplying $L_{ci}(z_1)$ and $U_{ci}(z_2)$ by $z^{-(N-1)/2}$ and $z_2^{-(N-1)/2}$, respectively.

A step-by-step procedure for the SVD-LUD realization starts with steps (1)–(4) given in Section III-A and concludes with the additional steps:

5a) Form coefficient matrix $\boldsymbol{C}$ using (11).

6a) Perform the LUD on matrix $\boldsymbol{C}$ to obtain matrices $\boldsymbol{L}_c$ and $\boldsymbol{U}_c$ by (16).

7a) Obtain the 2-D zero-phase transfer function through (17).

As in the modified-SVD realization, full accuracy can be achieved by using r_c parallel sections along with $K = r$, according to (15). The number of multiplications required in this realization is $K_c(2\bar{N} - K_c + 1)$, where $1 \leqslant K_c \leqslant r_c$, which is always less than $2K_c\bar{N}$, the number of multiplications required in the modified-SVD method. Also note that by (15), $K_c(2\bar{N} - K_c + 1)$, has an upper bound $\bar{N}(\bar{N}+1)$ which is less than $2\bar{N}^2$, the upper bound for the modified SVD method. Consequently, the SVD-LUD method usually leads to the most economical realization. The numbers of multiplications required by the three realization schemes are given in Table I.

TABLE I

Realizations	Direct SVD	Modified SVD	SVD-LUD
No. of Multipl	$2K\bar{N}$	$2K_c\bar{N}$	$K_c(2\bar{N} - K_c + 1)$
Upper Bound	$2r\bar{N}$	$2\bar{N}^2$	$\bar{N}(\bar{N}+1)$

IV. Error Analysis

As was demonstrated in Section III, in the direct-SVD realization a number of singular values of $\boldsymbol{A}$ and in the modified-SVD and SVD-LUD realizations a number of singular values of $\boldsymbol{A}$ and/or $\boldsymbol{C}$ may be neglected in practice. In this section, a quantitative error analysis is undertaken which would facilitate the determination of the number(s) of singular values that should be used in the design and the maximum approximation error that should be achieved in the design of the 1-D filters.

A. Direct-SVD Realization

Assume that the direct-SVD method has been used to design a 2-D FIR filter for a desired frequency response $\boldsymbol{A}$ and that its transfer function $H(z_1, z_2)$ is given by (2). Let $\tilde{\boldsymbol{f}}_i$ and $\tilde{\boldsymbol{g}}_i$ be the column vectors obtained by evaluating $\Phi_i(\omega_1)$ and $\Gamma_i(\omega_2)$ at frequencies $\omega_1 = \pi\mu_l/T_1$ and $\omega_2 = \pi\nu_m/T_2$, where $1 \leqslant l \leqslant L$ and $1 \leqslant m \leqslant M$, respectively, i.e.,

$$\tilde{\boldsymbol{f}}_i = \left[\Phi_i\left(\frac{\pi\mu_1}{T_1}\right) \cdots \Phi_i\left(\frac{\pi\mu_L}{T_1}\right)\right]^T$$

$$\tilde{\boldsymbol{g}}_i = \left[\Gamma_i\left(\frac{\pi\nu_1}{T_2}\right) \cdots \Gamma_i\left(\frac{\pi\nu_M}{T_2}\right)\right]^T.$$

The amplitude response of the 2-D filter at frequency point $(\omega_1, \omega_2) = (\pi\mu_l/T_1, \pi\nu_m/T_2)$ is given by $\sum_1^K \tilde{f}_i \tilde{g}_i^T$ and, therefore, the approximation error at this frequency point is the (l, m) entry in the error matrix $\boldsymbol{E}$ defined by

$$\begin{aligned} \boldsymbol{E} &= \{e_{l,m}\} \\ &= \sum_{i=1}^{K} \tilde{f}_i \tilde{g}_i^T - \boldsymbol{A} \\ &= \sum_{i=1}^{K} \left(\tilde{f}_i \tilde{g}_i^T - \tilde{\boldsymbol{u}}_i \tilde{\boldsymbol{v}}_i^T \right) - \sum_{i=K+1}^{r} \sigma_i \boldsymbol{u}_i \boldsymbol{v}_i^T. \end{aligned} \tag{18}$$

If we define

$$\Delta\tilde{\boldsymbol{u}}_i = \tilde{f}_i - \tilde{\boldsymbol{u}}_i;\ \Delta\tilde{\boldsymbol{v}}_i = \tilde{\boldsymbol{g}}_i - \tilde{\boldsymbol{v}}_i$$

then $\Delta\tilde{\boldsymbol{u}}_i$ and $\Delta\tilde{\boldsymbol{v}}_i$ represent the approximation errors in the 1-D frequency responses $\Phi_i(\omega_1)$ and $\Gamma_i(\omega_2)$, respectively. From (18), we can write

$$\begin{aligned} \boldsymbol{E} &= \sum_{i=1}^{K} \left(\Delta\tilde{\boldsymbol{u}}_i \tilde{\boldsymbol{v}}_i^T + \tilde{\boldsymbol{u}}_i \Delta\tilde{\boldsymbol{v}}_i^T + \Delta\tilde{\boldsymbol{u}}_i \Delta\tilde{\boldsymbol{v}}_i^T \right) - \sum_{i=K+1}^{r} \sigma_i \boldsymbol{u}_i \boldsymbol{v}_i^T \\ &= \sum_{i=1}^{K} \left[\sigma_i^{1/2} \left(\Delta\tilde{\boldsymbol{u}}_i \boldsymbol{v}_i^T + \boldsymbol{u}_i \Delta\tilde{\boldsymbol{v}}_i^T \right) + \Delta\tilde{\boldsymbol{u}}_i \Delta\tilde{\boldsymbol{v}}_i^T \right] - \sum_{i=K+1}^{r} \sigma_i \boldsymbol{u}_i \boldsymbol{v}_i^T. \end{aligned}$$

The (l, m) entry of matrix $\boldsymbol{E}$ can be expressed as

$$e_{l,m} = [p_1 \quad p_2 \quad \cdots \quad p_L] \boldsymbol{E} [q_1 \quad q_2 \quad \cdots \quad q_M]^T$$

where

$$p_i = \begin{cases} 1, & \text{for } i = l \\ 0, & \text{otherwise} \end{cases}$$

and

$$q_i = \begin{cases} 1, & \text{for } i = m \\ 0, & \text{otherwise} \end{cases}$$

and hence

$$e_{l,m} = \sum_{i=1}^{K} \left[\sigma_i^{1/2} \left(\Delta\tilde{u}_{il} v_{im} + u_{il} \Delta\tilde{v}_{im} \right) + \Delta\tilde{u}_{il} \Delta\tilde{v}_{im} \right] - \sum_{i=K+1}^{r} \sigma_i u_{il} v_{im}$$

where u_{il} denotes the lth component of vector $\boldsymbol{u}_i$, etc. Since vectors $\boldsymbol{u}_i$ and $\boldsymbol{v}_i$ are all unit vectors for $1 \leqslant i \leqslant r$, an upper bound on the magnitude of $e_{l,m}$ can be obtained as

$$|e_{l,m}| \leqslant \sum_{i=1}^{K} \left[\sigma_i^{1/2} (\epsilon_{1i} + \epsilon_{2i}) + \epsilon_{1i} \epsilon_{2i} \right] + \sum_{i=K+1}^{r} \sigma_i \tag{19}$$

where ϵ_{1i} and ϵ_{2i} represent the maximum approximation errors in the frequency responses $\Phi_i(\omega_1)$ and $\Gamma_i(\omega_2)$, respectively.

If the approximation error in each 1-D filter design is reasonably small, then the high-order terms $\epsilon_{1i}\epsilon_{2i}$, $1 \leqslant i \leqslant K$, in inequality (19) can be neglected. We note also that the right-hand side in (19) is independent of l and m, and hence (19) holds also for the maximum of $|e_{l,m}|$. We have, therefore, obtained an upper bound for the maximum approximation error over the set of sampled frequency points as

$$e_\infty = \max_{1 \leqslant l \leqslant L,\, 1 \leqslant m \leqslant M} |e_{l,m}| \leqslant \epsilon_{pK} + \epsilon_{rK} \tag{20}$$

where the principal error ϵ_{pK} and the residual error ϵ_{rK} are defined by

$$\epsilon_{pK} = \sum_{i=1}^{K} \sigma_i^{1/2} (\epsilon_{1i} + \epsilon_{2i}) \tag{21}$$

and

$$\epsilon_{rK} = \sum_{i=K+1}^{r} \sigma_i \tag{22}$$

respectively.

The error bound given by (20) shows clearly how the choice of K and the approximation error introduced by a specific 1-D design technique affect the overall approximation error in the 2-D filter. In practice, K should be chosen sufficiently small to keep the number of parallel sections small and the residual error ϵ_{rK} acceptable. Having determined the value of K, the principal error ϵ_{pK} can also be made acceptable by controlling the 1-D design errors ϵ_{1i} and ϵ_{2i} for $1 \leqslant i \leqslant K$, by increasing the orders of the 1-D filters or by using a better design method for the 1-D filters. From (21) it follows that small approximation error should be obtained in the design of those 1-D filters that correspond to the large singular values.

B. Modified-SVD and SVD-LUD Realizations

As in the direct-SVD realization, a trade-off exists between the number of parallel sections used and the approximation error. An error analysis is, therefore, useful to the designer.

Assume that a 2-D FIR filter has been designed using K singular values of the desired frequency response $\boldsymbol{A}$ and that its transfer function $H(z_1, z_2)$ is given by (10). If a modified-SVD or a SVD-LUD realization is obtained comprising K_c parallel sections, where $1 \leqslant K_c \leqslant r_c$, the error introduced is given from (10) and (14) as

$$H(z_1, z_2) - \hat{H}(z_1, z_2) = \boldsymbol{Z}_1 \left(\sum_{i=K_c+1}^{r_c} \sigma_{ci} \boldsymbol{u}_{ci} \boldsymbol{v}_{ci}^T \right) \boldsymbol{Z}_2^T \tag{23}$$

where $\boldsymbol{Z}_i$, $i = 1, 2$, are row vectors as defined in Section III-C and

$$\begin{aligned} \hat{H}(z_1, z_2) &= \boldsymbol{Z}_1 \left(\sum_{i=1}^{K_c} \sigma_{ci} \boldsymbol{u}_{ci} \boldsymbol{v}_{ci}^T \right) \boldsymbol{Z}_2^T \\ &= \sum_{i=1}^{K_c} \tilde{F}_{ci}(z_1) \tilde{G}_{ci}(z_2). \end{aligned}$$

Under these circumstances, the approximation error at frequency point $(\omega_1, \omega_2) = (\pi\mu_l/T_1, \pi\nu_m/T_2)$ is given by

$$\begin{aligned} |\hat{e}_{l,m}| &= |a_{l,m} - \hat{H}(e^{j\omega_1 T_1}, e^{j\omega_2 T_2})| \\ &\leqslant |a_{l,m} - H(e^{j\omega_1 T_1}, e^{j\omega_2 T_2})| \\ &\quad + |H(e^{j\omega_1 T_1}, e^{j\omega_2 T_2}) - \hat{H}(e^{j\omega_1 T_1}, e^{j\omega_2 T_2})| \\ &\leqslant |e_{l,m}| + |H(e^{j\omega_1 T_1}, e^{j\omega_2 T_2}) - \hat{H}(e^{j\omega_1 T_1}, e^{j\omega_2 T_2})| \end{aligned} \tag{24}$$

where $|e_{l,m}|$ has an upper bound given by (20) and by (23) the second term on the right-hand side in (24) can be estimated as

$$
\begin{aligned}
|H(e^{j\omega_1 T_1}, e^{j\omega_2 T_2}) - \hat{H}(e^{j\omega_1 T_1}, e^{j\omega_2 T_2})| &= \left| Z_1 \left(\sum_{i=K_c+1}^{r_c} \sigma_{ci} u_{ci} v_{ci}^T \right) Z_2^T \right| \\
&\leqslant \|Z_1\| \, \|Z_2\| \left\| \left(\sum_{i=K_c+1}^{r_c} \sigma_{ci} u_{ci} v_{ci}^T \right) \right\| \\
&\leqslant N \sum_{i=k_c+1}^{r_c} \sigma_{ci}
\end{aligned}
\tag{25}
$$

where $\|\cdot\|$ denotes the Euclidean norm of the matrix involved. The estimate in (24) in conjunction with (20) and (25) leads to

$$\hat{e}_\infty = \max_{1 \leqslant l \leqslant L,\, 1 \leqslant m \leqslant M} |\hat{e}_{l,m}| \leqslant \epsilon_{pK} + \epsilon_{rK} + \epsilon_s \tag{26}$$

where ϵ_{pK} and ϵ_{rK} are given by (21) and (22), respectively, and ϵ_s given by

$$\epsilon_s = N \sum_{i=K_c+1}^{r_c} \sigma_{ci} \tag{27}$$

is the error introduced by using a reduced number of sections.

With $K = r$, the residual error in (26) vanishes and (26) becomes

$$\hat{e}_\infty \leqslant \epsilon_{pr} + \epsilon_s. \tag{28}$$

In other words, one can design a linear-phase 2-D FIR digital filter using only K_c parallel sections if all the 1-D filters involved are designed such that the principal error ϵ_{pr} is sufficiently small and, if K_c is chosen such that the error in (27) is also sufficiently small.

V. Examples

In this section, the design of a bandpass and a fan 2-D filter are presented to illustrate the effectiveness of the proposed design method.

Example 1

The desired amplitude response of a circularly-symmetric 2-D bandpass FIR filter is specified by

$$|H_1(e^{j\omega_1 T_1}, e^{j\omega_2 T_2})| = \begin{cases} 0, & 0 \leqslant \sqrt{\omega_1^2 + \omega_2^2} \leqslant \omega_{a1} \\ 1, & \omega_{p1} \leqslant \sqrt{\omega_1^2 + \omega_2^2} \leqslant \omega_{p2} \\ 0, & \omega_{a2} \leqslant \sqrt{\omega_1^2 + \omega_2^2} \leqslant \pi \end{cases}$$

where $\omega_{a1} = 0.24\pi$, $\omega_{p1} = 0.36\pi$, $\omega_{p2} = 0.64\pi$, and $\omega_{a2} = 0.76\pi$ and is illustrated in Fig. 1. The corresponding sampled amplitude response $A_1 = |H_1(e^{j\pi\mu_l}, e^{j\pi\nu_m})|$ using $L = M = 36$ can be expressed as

$$|H_1(e^{j\pi\mu_l}, e^{j\pi\nu_m})| = \begin{cases} 0, & 0 \leqslant \sqrt{\mu_l^2 + \nu_m^2} < \omega_{c1}/\pi \\ 1, & \omega_{c1}/\pi \leqslant \sqrt{\mu_l^2 + \nu_m^2} \leqslant \omega_{c2}/\pi \\ 0, & \omega_{c2}/\pi < \sqrt{\mu_l^2 + \mu_m^2} \leqslant 1 \end{cases}$$

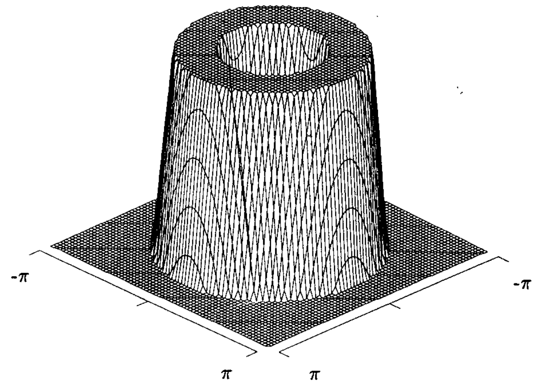

Fig. 1. Ideal amplitude response of 2-D FIR bandpass digital filter.

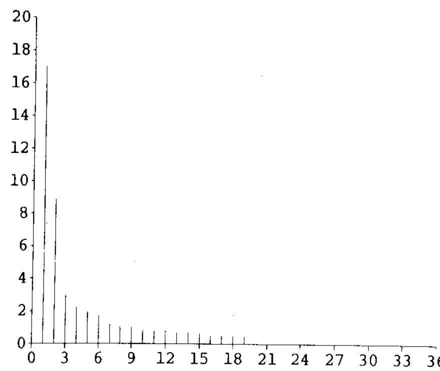

Fig. 2. Singular-value distribution of matrix A_1.

where

$$\omega_{c1} = (1/2)(\omega_{a1} + \omega_{p1}); \quad \omega_{c2} = (1/2)(\omega_{a2} + \omega_{p2}).$$

An easy-to-use numerically reliable software package called MATLAB has been used to perform SVD on matrix A_1 in order to obtain the necessary data for the designs in the following steps.

The 1-D FIR filters were designed by using the Fourier series method along with the Kaiser window function, which is known for its flexibility [7]. As may be expected, the higher the order of the 1-D filters, the lower the approximation error. By trial and error, a value of 29 for N was found to give satisfactory results.

As is shown in Fig. 2, there are 19 nonzero singular values resulting from the SVD of matrix A_1 but only the first 9 are significant. The 3-D plot and the contour plot of the amplitude response obtained for a direct-SVD realization with 9 sections are shown in Fig. 3(a) and (b) (each contour plot used in this paper has 12 levels), respectively.

If all 19 nonzero singular values of A_1 are used in the design, then the rank of matrix C defined in (11) is 15. However, only 9 singular values of C are significant and the digital filter can be realized using the modified-SVD or SVD-LUD scheme with $K_c = 9$. The 3-D plot and the contour plot of the amplitude response obtained are shown in Fig. 4(a) and (b), respectively. The maximum passband and stopband errors for different values of K and K_c are

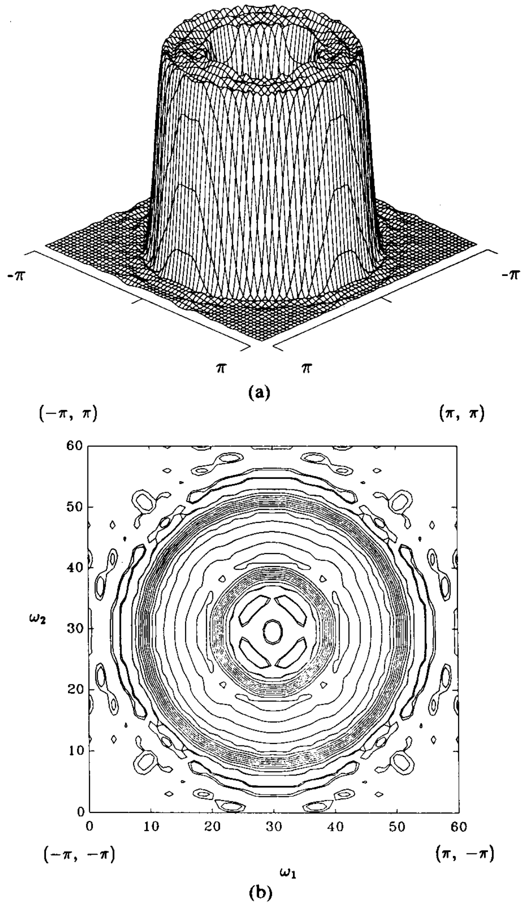

Fig. 3. Amplitude response of bandpass filter using the direct-SVD realization with $K = 9$. (a) 3-D plot. (b) Contour plot.

shown in Table II. The number of multiplications required by the three realization schemes are listed in Table III. An examination of Tables II and III suggests that the best choice for the designer is to use $K = 19$ and $K_c = 9$, and realize the filter by the SVD-LUD scheme.

Example 2

The above approach has also been applied for the design of a fan filter having an amplitude response

$$|H_2(e^{j\omega_1 T_1}, e^{j\omega_2 T_2})| = \begin{cases} 1, & \omega_2 < 0.6\omega_1 - 0.02857\pi \\ 0, & \omega_2 > 0.6\omega_1 + 0.1143\pi \end{cases}$$

for $0 \leqslant \omega_1, \omega_2 \leqslant \pi$, as depicted in Fig. 5. The corresponding sampled amplitude response $A_2 = |H_2(e^{j\pi\mu_l}, e^{j\pi\nu_m})|$ with $L = M = 36$ can be written as

$$|H_2(e^{j\pi\mu_l}, e^{j\pi\nu_m})| = \begin{cases} 1, & \nu_m < 0.6\mu_l + 0.0457 \\ 0, & \nu_m \geqslant 0.6\mu_l + 0.0457 \end{cases}.$$

There are 22 nonzero singular values resulting from the SVD of matrix A_2 as depicted in Fig. 6 but only the first 9 are significant. The amplitude response obtained for a direct-SVD realization with $K = 9$ is illustrated in Fig. 7(a) and (b).

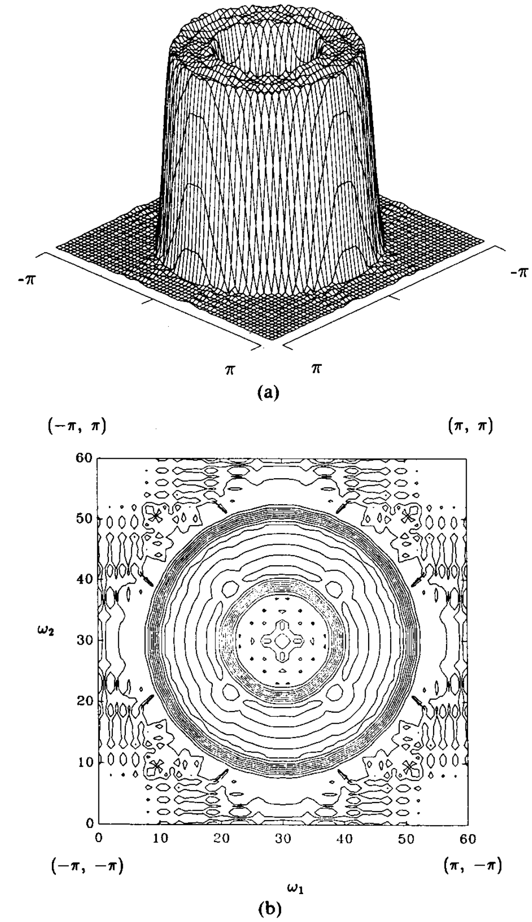

Fig. 4. Amplitude response of bandpass filter using the modified-SVD or SVD-LUD realization with $K = 19$ and $K_c = 9$. (a) 3-D plot. (b) Contour plot.

TABLE II

	Direct SVD			Modified SVD or SVD-LUD
K	9	15	19	$K = 19, K_c = 9$
Max. Passband Error	0.0332	0.0276	0.0275	0.0282
Max. Stopband Error	0.0290	0.0287	0.0263	0.0274

TABLE III

K	Direct SVD	Modified SVD		SVD-LUD	
		$K_c = 9$	$K_c = 15$	$K_c = 9$	$K_c = 15$
9	270	270	N/A	198	N/A
15	450	270	450	198	240
19	570	270	450	198	240
22	660	270	450	198	240

If all 22 nonzero singular values of A_2 are used in the design, then the rank of matrix C defined in (11) is 15 but only 9 singular values of C are significant. Therefore, the digital filter can be realized using the modified-SVD or SVD-LUD realization scheme with $K_c = 9$. The amplitude response obtained is illustrated in Fig. 8(a) and (b). The maximum passband and stopband errors for different values of K and K_c are shown in Table IV. The number of

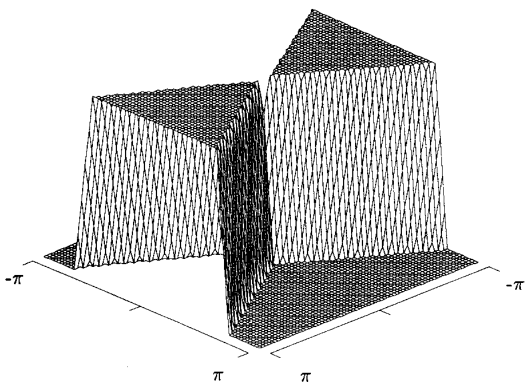

Fig. 5. Ideal amplitude response of 2-D FIR fan digital filter.

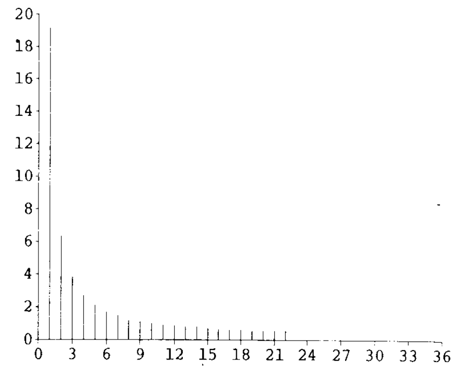

Fig. 6. Singular-value distribution of matrix A_2.

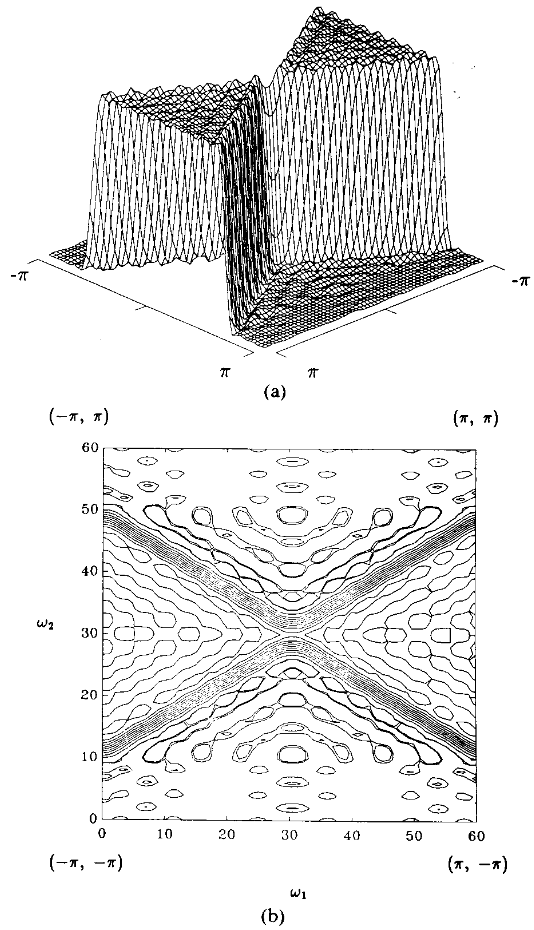

Fig. 7. Amplitude response of fan filter using the direct-SVD realization with $K = 9$. (a) 3-D plot. (b) Contour plot.

multiplications required by the three realization schemes are given in Table III. An examination of Tables IV and III suggests that the best choice for the designer is to use $K = 22$, $K_c = 9$ and realize the filter by the SVD-LUD scheme.

VI. Comparisons

To compare the proposed design method with other well-established design methods, the McClellan transformation method [10], [11] and the 2-D window method [12] have been used to design the same bandpass and fan filters.

A 1-D bandpass FIR filter of order 29 was first designed and the linear McClellan transformation recommended in [10] was then used to obtain a 29×29 2-D, circularly-symmetric, bandpass filter. The amplitude response obtained is illustrated in Fig. 9(a) and (b). The application of the window method gives a 29×29 bandpass filter whose amplitude response is illustrated in Fig. 10(a) and (b).

The maximum passband and stopband errors obtained are summarized in Table V along with the results obtained in the SVD-LUD realization with $K = 19$ and $K_c = 9$. As can be seen, the SVD approach gave the lowest approximation error with respect to the passband and stopbands and resulted, in addition, in highly circular contours in the amplitude response. The window method gave a fairly good approximation but a relatively large number of multiplications is required in the implementation. The McClellan transformation, on the other hand, resulted in the most economical realization [13] but, unfortunately, the approximation error is quite large in the upper stopband. Furthermore, the circularity of the contours of the amplitude response deteriorates rapidly as ω_1 and ω_2 are increased.

The McClellan transformation and window method were then used to design the fan filter of Example 2. The amplitude responses achieved are shown in Figs. 11 and 12, respectively. The results obtained are summarized in Table VI along with the results obtained in the SVD-LUD realization with $K = 22$ and $K_c = 9$. Evidently, these results are fairly consistent with those in Table V and one is, therefore, tempted to conclude that the aforementioned merits and demerits of the three approaches are applicable to other types of filters.

VII. Conclusions

The SVD has been applied in the design of 2-D FIR digital filters and three realizations have been proposed. The direct-SVD realization is based on the principles used in [3] for the design of 2-D IIR filters. However, the

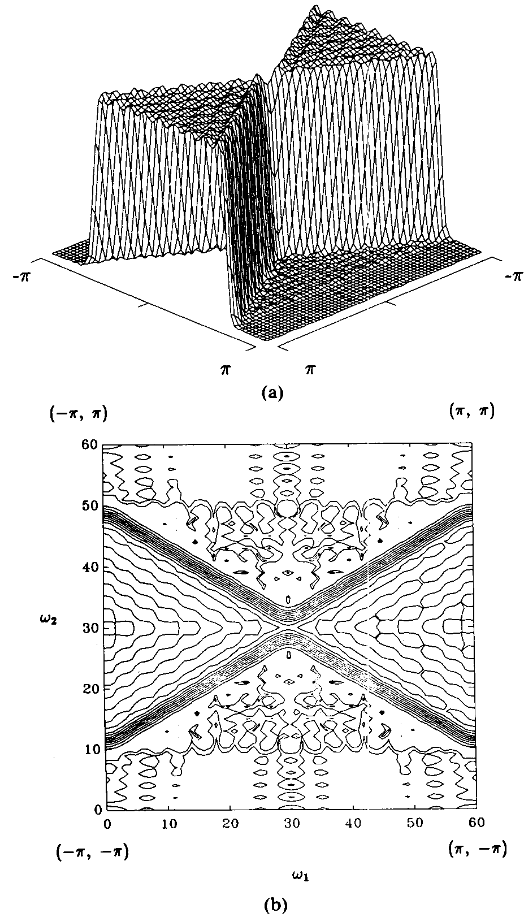

Fig. 8. Amplitude response of fan filter using the modified-SVD or SVD-LUD realization with $K = 22$ and $K_c = 9$. (a) 3-D plot. (b) Contour plot.

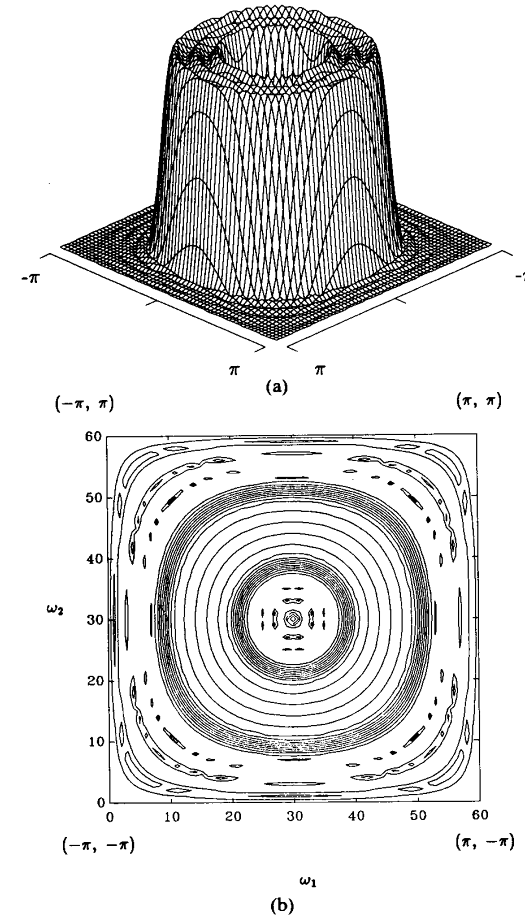

Fig. 9. Amplitude response of bandpass filter using the McClellan transformation method. (a) 3-D plot. (b) Contour plot.

TABLE IV

	Direct SVD			Modified SVD or SVD-LUD
K	9	15	22	$K = 22,\ K_c = 9$
Max. Passband Error	0.0475	0.0391	0.0390	0.0411
Max. Stopband Error	0.0331	0.0267	0.0250	0.0281

modified-SVD and SVD-LUD realizations are, to the knowledge of the authors, new.

Each of the three realizations consists of a parallel arrangement of cascaded pairs of 1-D digital filters. Hence extensive parallel processing and pipelining can be applied. The 1-D FIR filters can be designed using well-known standard design methods and by using linear-phase causal 1-D filters, linear-phase causal 2-D filters can be obtained.

A quantitative error analysis has been carried out which can facilitate the determination of K and K_c, the numbers of singular values of matrices $\boldsymbol{A}$ and $\boldsymbol{C}$, that should be used in the design and the maximum approximation error that should be achieved in the design of the 1-D filters.

The three realizations were used to design a bandpass and a fan filter and the results obtained were compared. It was found that when the same number of parallel sections are used in the three realizations, the modified-SVD realization results in a smaller approximation error than the direct-SVD realization and the SVD-LUD realization results in the same approximation error as the modified-SVD realization but requires a reduced number of multiplications. Therefore, the SVD-LUD realization is the best of the three and should always be preferred. However, this does not obviate the need for the other two realizations since the direct-SVD realization must be obtained before the modified-SVD realization can be obtained and, in turn, the modified-SVD realization must be obtained before the SVD-LUD realization can be obtained.

The bandpass and fan filters were also designed using the McClellan transformation and the 2-D window method and the results obtained were compared with the results obtained using the SVD approach. The SVD-LUD realization resulted in very good approximations both with respect to the passband and stopband(s) while the computational complexity was moderate in both examples; in the case of the bandpass filter, excellent contour circularity was achieved in the passband. The 2-D window method

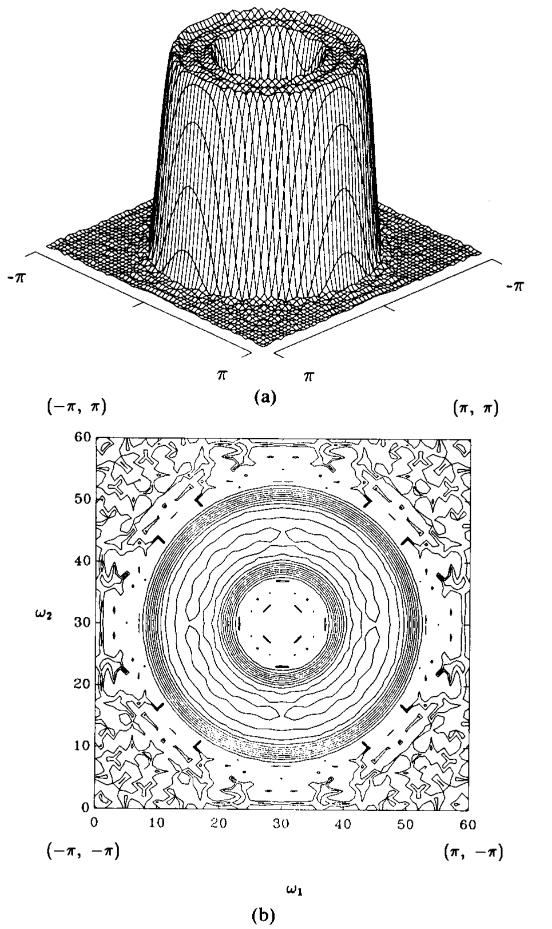

Fig. 10. Amplitude response of bandpass filter using the window method. (a) 3-D plot. (b) Contour plot.

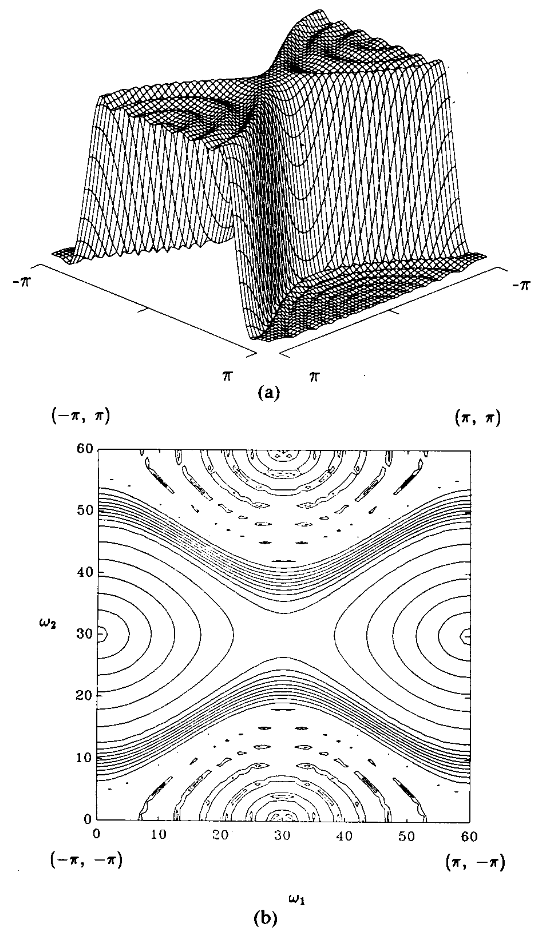

Fig. 11. Amplitude response of fan filter using the McClellan transformation method. (a) 3-D plot. (b) Contour plot.

resulted in fairly good approximations but the number of multiplications required in each design was very high. The McClellan transformation resulted in the most economical designs but the approximation error was found to be quite large in the upper stopband of the bandpass filter and the stopband of the fan filter; in addition, in the bandpass filter the circularity of the contours was found to deteriorate at higher frequencies.

Appendix A

Let $C = \{c_{i,j},\ 0 \leqslant i,\ j \leqslant N-1,\ N = \text{odd}\}$ be an $N \times N$ quadrantally-symmetric matrix, i.e.,

$$c_{i,j} = c_{i,N-1-j} = c_{N-1-i,j} = c_{N-1-i,N-1-j}. \tag{A.1}$$

If a matrix $\hat{I}$ is defined by

$$\hat{I} = \begin{bmatrix} 0 & \cdots & 0 & 1 & 0 \\ 0 & \cdots & 1 & 0 & 0 \\ \vdots & \vdots & \vdots & \vdots & \vdots \\ 1 & \cdots & 0 & 0 & 0 \end{bmatrix} \tag{A.2}$$

where the size of $\hat{I}$ is $l \times k$, and $k = (N+1)/2$, $l = (N-1)/2$, then matrix C can be decomposed as

$$C = \begin{bmatrix} I_k & 0 \\ \hat{I} & I_l \end{bmatrix} \begin{bmatrix} C_1 & 0 \\ 0 & 0 \end{bmatrix} \begin{bmatrix} I_k & \hat{I}^T \\ 0 & I_l \end{bmatrix} \tag{A.3}$$

where C_1 is the $k \times k$ principal minor of C. Assume that the SVD of matrix C_1 is given by

$$C_1 = U_1 S_1 V_1^T. \tag{A.4}$$

From (A.3) and (A.4), matrix C can be expressed as

$$\begin{aligned} C &= \begin{bmatrix} U_1 & 0 \\ \hat{I}U_1 & 0 \end{bmatrix} \begin{bmatrix} S_1 & 0 \\ 0 & 0 \end{bmatrix} \begin{bmatrix} V_1 & 0 \\ \hat{I}V_1 & 0 \end{bmatrix}^T \\ &= \left(\frac{1}{\sqrt{2}} \begin{bmatrix} U_1 & 0 \\ \hat{I}U_1 & 0 \end{bmatrix} \right) \begin{bmatrix} 2S_1 & 0 \\ 0 & 0 \end{bmatrix} \left(\frac{1}{\sqrt{2}} \begin{bmatrix} V_1 & 0 \\ \hat{I}V_1 & 0 \end{bmatrix}^T \right) \\ &= \begin{bmatrix} \bar{U}_1 & 0 \end{bmatrix} \begin{bmatrix} 2S_1 & 0 \\ 0 & 0 \end{bmatrix} \begin{bmatrix} \bar{V}_1 & 0 \end{bmatrix} \end{aligned} \tag{A.5}$$

where

$$\bar{U}_1 = \frac{1}{\sqrt{2}} \begin{bmatrix} U_1 \\ \hat{I}U_1 \end{bmatrix} \quad \text{and} \quad \bar{V}_1 = \frac{1}{\sqrt{2}} \begin{bmatrix} V_1 \\ \hat{I}V_1 \end{bmatrix}. \tag{A.6}$$

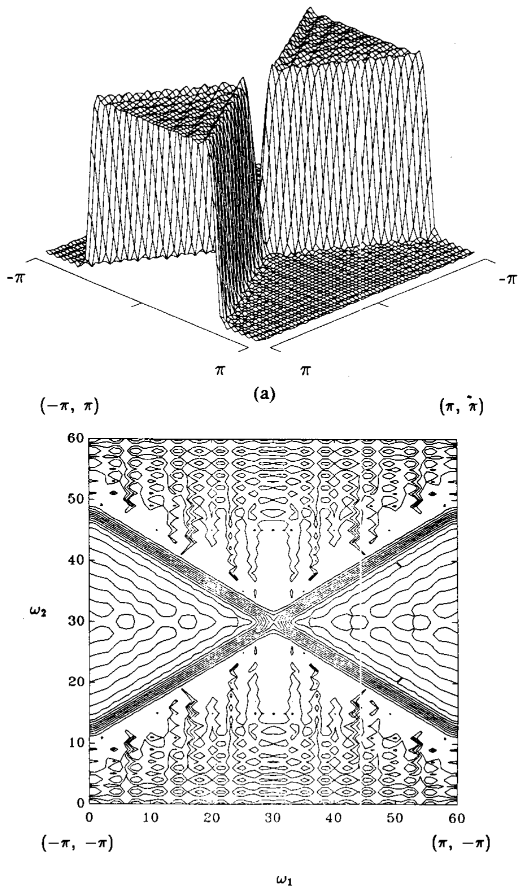

Fig. 12. Amplitude response of fan filter using the window method. (a) 3-D plot. (b) Contour plot.

TABLE V

	SVD-LUD realization with $K = 19$, $K_c = 9$	McClellan method	Window method
Max. Passband Error	0.0262	0.0381	0.0281
Max. Stopband Error	0.0274	0.3709	0.0714
No. of Multipl.	198	169	240

TABLE VI

	SVD-LUD realization with $K = 22$, $K_c = 9$	McClellan method	Window method
Max. Passband Error	0.0411	0.0325	0.2905
Max. Stopband Error	0.0281	0.9634	0.0220
No. of Multipl	198	169	240

If $\overline{U}_2$ and $\overline{V}_2$ are the orthonormal complements of $\overline{U}_1$ and $\overline{V}_1$, respectively, then the SVD of matrix C can be obtained from (A.5) as

$$C = USV^T = \sum_{i=1}^{r_c} \sigma_i \boldsymbol{u}_i \boldsymbol{v}_i^T = \sum_{i=1}^{r_c} \tilde{\boldsymbol{u}}_i \tilde{\boldsymbol{v}}_i^T \tag{A.7}$$

where $U = [\overline{U}_1 \;\; \overline{U}_2]$ and $V = [\overline{V}_1 \;\; \overline{V}_2]$ are orthogonal matrices, $\boldsymbol{u}_i$ and $\boldsymbol{v}_i$ represent the ith column of U and V, respectively, $\tilde{\boldsymbol{u}}_i = \sigma_i^{1/2}\boldsymbol{u}_i$, $\tilde{\boldsymbol{v}}_i = \sigma_i^{1/2}\boldsymbol{v}_i$ and

$$S = \begin{bmatrix} 2S_1 & \mathbf{0} \\ \mathbf{0} & \mathbf{0} \end{bmatrix} = \begin{bmatrix} \sigma_1 & 0 & \cdots & & & & 0 \\ 0 & \sigma_2 & 0 & \cdots & & & 0 \\ \vdots & \cdots & \sigma_{rc} & 0 & \cdots & & \vdots \\ & \cdots & \cdots & 0 & \cdots & & \\ & \cdots & & \vdots & & & 0 \\ 0 & \cdots & & & & & 0 \end{bmatrix}.$$

From (A.2) and (A.6), we now observe that the first k columns of U and V are all mirror-image symmetric and, consequently, the vectors $\tilde{\boldsymbol{u}}_i$ and $\tilde{\boldsymbol{v}}_i$ in (A.7) are all mirror-image symmetric.

Appendix B

If the LUD of matrix C_1 is given by

$$C_1 = L_1 U_1 \tag{B.1}$$

where L_1 and U_1 are lower and upper triangular matrices of size N_1, then (A.1) implies that

$$C = \begin{bmatrix} I_k & \mathbf{0} \\ \hat{I} & I_l \end{bmatrix} \begin{bmatrix} L_1 & \mathbf{0} \\ \mathbf{0} & \mathbf{0} \end{bmatrix} \begin{bmatrix} U_1 & \mathbf{0} \\ \mathbf{0} & \mathbf{0} \end{bmatrix} \begin{bmatrix} I_k & \hat{I}^T \\ \mathbf{0} & I_l \end{bmatrix} = \begin{bmatrix} L_1 & \mathbf{0} \\ \hat{I}L_1 & \mathbf{0} \end{bmatrix} \begin{bmatrix} U_1 & U_1\hat{I}^T \\ \mathbf{0} & \mathbf{0} \end{bmatrix}$$

and, therefore, the LUD of C is given by

$$C = L_c U_c$$

where L_c and U_c are of the form given in Section III-C.

References

[1] S. Treitel and J. L. Shanks, "The design of multistage separable planar filters," *IEEE Trans. Geosci. Electron.*, vol. GE-9, pp. 10–27, Jan. 1971.

[2] R. E. Twogood and S. K. Mitra, "Computer-aided design of separable two-dimensional digital filters," *IEEE Trans. Acoust., Speech, Signal Processing*, vol. ASSP-25, pp. 165–169, Apr. 1977.

[3] A. Antoniou and W.-S. Lu, "Design of two-dimensional digital filters by using the singular value decomposition," *IEEE Trans. Circuits Syst.*, vol. CAS-34, pp. 1191–1198, Oct. 1987.

[4] A. N. Venetsanopoulos and C. L. Nikias, "Realization of two-dimensional digital filters by LU decomposition of their transfer function," in *Proc. IEEE Int. Conf. Acoust., Speech, Signal Processing*, San Diego, CA, pp. 20.4.1–20.4.4, Mar. 1984.

[5] P. Karivaratharajan and M. N. S. Swamy, "Realization of a 2-dimensional FIR digital filter using separable filters," *Electron. Lett.*, vol. 14, no. 8, pp. 294–251, Apr. 1978.

[6] B. R. Suresh and B. A. Shenoi, "Exact realization of 2-dimensional digital filters by separable filters," *Electron. Lett.*, vol. 12, no. 10, pp. 242–244, 1976.

[7] A. Antoniou, *Digital Filters: Analysis and Design*. New York: McGraw-Hill, 1979.

[8] T. W. Parks and J. H. McClellan, "Chebyshev approximation for nonrecursive digital filters with linear phase," *IEEE Trans. Circuits Theory*, vol. CT-19, pp. 189–194, Mar. 1972.

[9] G. H. Golub and C. F. Van Loan, *Matrix Computations*. Baltimore, MD: The Johns Hopkins Univ. Press, 1983.

[10] R. M. Mersereau, W. F. G. Mecklenbrauker, and T. F. Quatieri, Jr., "McClellan transformations for two-dimensional digital filtering: I —Design" *IEEE Trans. Circuits Syst.*, vol. CAS-23, pp. 405–413, July 1976.

[11] D. E. Dudgeon and R. M. Mersereau, *Multidimensional Digital Signal Processing*. Englewood Cliffs, NJ: Prentice-Hall, 1984.

[12] T. S. Huang, "Two-dimensional windows," *IEEE Trans. Audio Electroacoust.*, vol. AU-20, pp. 88–89, Mar. 1972.

[13] J. H. McClellan and D. S. K. Chen, "A 2-D filter structure derived from the Chebyshev recursion," *IEEE Trans. Circuits Syst.* vol. CAS-24, pp. 372–378, July 1977.

Wu-Sheng Lu (S'82–M'85) received the M.S. degree in electrical engineering and the Ph.D. degree in control science from the University of Minnesota in 1983 and 1984, respectively.

He was a Post-Doctoral Fellow at the University of Victoria, Victoria, B.C., Canada, in 1985 and held a visiting position at the University of Minnesota in 1986. Since 1987, he has been with the Department of Electrical and Computer Engineering, University of Victoria, B.C., Canada where he is currently Associate Professor. His research interests include digital signal processing, control, and robotics.

Hui-Ping Wang (S'88) received the B.Eng. degree from Beijing University of Posts and Telecommunications, Beijing, China, in 1984 and the M.A.S. degree in 1987 from the University of Victoria, Victoria, B.C., Canada, where she is currently working toward the Ph.D. degree in electrical engineering.

While at U.Vic, she has been working as a research and teaching assistant, and has received University of Victoria Fellowships during the period 1986–1989 and the Charles S. Humphrey Awards for 1986–1987 and 1987–1988. Her research interests are in the areas of multidimensional digital signal processing and VLSI implementations of algorithms.

Andreas Antoniou (M'69–SM'79–F'82) received the B.Sc. (Eng.) and Ph.D. degrees in electrical engineering from London University, London, U.K., in 1963 and 1966, respectively.

From 1966 to 1969, he was Senior Scientific Officer at the Post Office Research Department, London, U.K., and from 1969 to 1970, he was a member of the Scientific Staff at the R&D Laboratories of Northern Electric Company Ltd., Ottawa, Ont., Canada. From 1970 to 1983, he served in the Department of Electrical Engineering, Concordia University, Montreal, Quebec, Canada, as Professor from June 1973 and as Chairman from December 1977. On July 1, 1983 he was appointed founding Chairman of the Department of Electrical Engineering, University of Victoria, Victoria, B.C., Canada. His teaching and research interests are in the areas of electronics, network synthesis, digital system design, active and digital filters, and digital signal processing. He has published a number of papers on electronic circuits, active filters, and digital filters. He authored *Digital Filters: Analysis and Design*, (New York: McGraw-Hill). One of his papers on gyrator circuits was awarded the Ambrose Fleming Premium by the Institution of Electrical Engineers, UK. He was Associate Editor, IEEE TRANSACTIONS ON CIRCUITS AND SYSTEMS during the period June 1983 to May 1985 and Editor of the same TRANSACTIONS during the period June 1985 to May 1987. He served as Technical Program Chairman of the 1989 IEEE International Symposium on Circuits and Systems.

Dr. Antoniou is a Member and, at present, a Counsellor of the Association of Professional Engineers of British Columbia, Canada.